Infection, Genetics and Evolution 23 (2014) 106–114

Contents lists available at ScienceDirect

Infection, Genetics and Evolution

journal homepage: www.elsevier.com/locate/meegid

Origin and distribution of AT-rich repetitive DNA families in *Triatoma infestans* (Heteroptera)

Vanessa Bellini Bardella [a], João Aristeu da Rosa [b], André Luís Laforga Vanzela [c,*]

[a] Departamento de Biologia, Instituto de Biociências, Letras e Ciências Exatas, IBILCE/UNESP, 15054-000 São José do Rio Preto, São Paulo, Brazil
[b] Departamento de Ciências Biológicas, Faculdade de Ciências Famacêuticas de Araraquara, FCFAR/UNESP, 14801-902 Araraquara, São Paulo, Brazil
[c] Departamento de Biologia Geral, CCB, Universidade Estadual de Londrina, 86051-990 Londrina, Paraná, Brazil

ARTICLE INFO

Article history:
Received 21 November 2013
Received in revised form 26 January 2014
Accepted 29 January 2014
Available online 10 February 2014

Keywords:
Heterochromatin
Holocentric chromosomes
Immunolabeling
Molecular cytogenetic
SatDNA
Reduviidae

ABSTRACT

Triatoma infestans, one of the most important vectors of *Trypanosoma cruzi*, is very interesting model, because it shows large interpopulation variation in the amount and distribution of heterochromatin. This polymorphism involved the three large pairs up to almost all autosomal pairs, including the sex chromosomes. To understand the dynamics of heterochromatin variation in *T. infestans*, we isolated the AT-rich satDNA portion of this insect using reassociation kinetics (C_0t), followed by cloning, sequencing and FISH. After chromosome localization, immunolabeling with anti-5-methylcytosine, anti-H4K5ac and anti-H3K9me2 antibodies was performed to determine the functional characteristics of heterochromatin. The results allowed us to reorganize the karyotype of *T. infestans* in accordance with the distribution of the families of repetitive DNA using seven different markers. We found that two arrays with lengths of 79 and 33 bp have a strong relationship with transposable element sequences, suggesting that these two families of satDNA probably originated from Polintons. The results also allowed us to identify at least four chromosome rearrangements involved in the amplification/dispersion of AT-rich satDNA of *T. infestans*. These data should be very useful in new studies including those examining the cytogenomic and population aspects of this very important species of insect.

1. Introduction

Heterochromatin is known as a nuclear fraction with high methylation/condensation state, low functional activity, late replication and lower susceptibility to recombination events. These characteristics are common in regions rich of repetitive DNA families, such as satDNA, and they can vary between species in size, composition and amount of motifs (Schmidt and Heslop-Harrison, 1998; Subirana and Messeguer, 2013). This diversity of heterochromatic regions can be exemplified by proximal chromosome regions of some coleopterans, whose composition of repetitive DNA families depends on the species or group of species. *Palorus subdepressus*, for instance, shows an array with a length of 72 bp, tandemly repeated in the pericentromeric region, whose sequence is also found in other coleopterans, such as *Chysolina americana* (Plohl et al., 1998; Lorite et al., 2001). In Aphididae, a family of Hemiptera with holokinetic chromosomes, three families of repetitive DNA were found: (i) an array of 3.000 bp length associated with a terminal GC-rich region in the X chromosome, (ii) a 200 bp length sequence associated with an AT-rich region of X chromosome, and (iii) a satDNA obtained after *Hae*III cleavage associated with AT-rich regions of autosomes (Mandrioli et al., 1999).

The traditional methods of chromosome banding (C-Giemsa and CMA_3/DAPI) have been useful for revealing the location, size and AT- or GC-rich composition of heterochromatic regions in the chromosomes and nucleus, and also for producing markers to compare karyotypes of different species and/or groups of insects (Schneider et al., 2006; Bressa et al., 2008; Cabral-de-Mello et al., 2010; Panzera et al., 2010; Bardella et al., 2014). Especially for Triatominae, chromosome banding allows us to identify intra- and interspecific variations in the amount and distribution of

Abbreviations: TRF, tandem repeats finder; TIRs, Terminal Inverted Repeats; SSC, saline-sodium citrate; SDS, sodium dodecyl sulfate; FITC, fluorescein isothiocyanate; DABCO, 1,4-diazabicyclo[2.2.2]octane; PBS, phosphate-buffered saline; BSA, bovine serum albumin; TRITC, tetramethylrhodamine-5-(and-6-)isothiocyanate; FISH, fluorescence in situ hybridization; HCl, hydrochloric acid; CMA_3, chromomycin A_3; DAPI, 4′-6-diamidino-2-phenylindole; Tris, tris(hydroxymethyl)aminomethane hydrochloride; $MgCl_2$, magnesium chloride; NCBI, National Center of Biotechnology Information.

* Corresponding author. Tel.: +55 43 33714417.
E-mail addresses: vanessabellini@ig.com.br (V.B. Bardella), joaoaristeu@gmail.com (J.A. da Rosa), andrevanzela@uel.br (A.L.L. Vanzela).

http://dx.doi.org/10.1016/j.meegid.2014.01.035
1567-1348/

heterochromatin (Panzera et al., 1992, 1995). An example is the intraspecific polymorphism of chromosome band patterns between natural populations of *Triatoma infestans* (Panzera et al., 1992, 1995). Panzera et al. (2004) suggested that Andean population of *T. infestans* exhibit heterochromatin in 14–20 chromosomes, and about 1.825 ± 0.49 pg per haploid nucleus. However, non-Andean populations seems to be from four to seven chromosomes carrying bands and a *C*-value with about 1.401 ± 0.111 pg. These data suggested that polymorphisms were associated with migration and adaptation of genomes during the occupation of this species in new environments in South America. Karyotype changes were also observed in the distribution of 18S rDNA in distinct population of *T. infestans*, whose hybridization signals can occur in autosomes or alosomes (Panzera et al., 2012).

Triatoma infestans has holokinetic chromosomes and $2n = 20 + XY$, like the majority of species of Triatominae (Ueshima, 1979; Panzera et al., 1996). Karyotypes of *T. infestans* are asymmetrically organized into three large pairs and the remainder smaller pairs, with the Y chromosome always larger than X in the non-Andean group (Pérez et al., 2000), because the X not have C-heterochromatin. But in Andean group, both sex chromosomes are similar in size and both of them have C-heterochromatin (Panzera et al., 2004). This species is also particularly intriguing because it belongs to a hematophagous insect group that is important to public health in Latin America, because they are the main vectors of the parasite *Trypanosoma cruzi*, responsible for Chagas disease. According to the World Health Organization (http://www.who.int/topics/chagas_disease/en/), approximately 10 million people were infected with *T. cruzi* in 2012.

To understand the origin and variation of heterochromatic regions in *T. infestans*, we used C_0t DNA reassociation to isolate and to produce a plasmid microlibrary with short DNA fragments, followed by cloning and SANGER sequencing. This strategy was useful in selecting different repetitive DNA fragments for physical mapping. The main goal of this study was to determine the mechanisms that account for the origin, distribution and diversity of AT-rich heterochromatin that occupy predominantly the terminal chromosome regions.

2. Materials and methods

2.1. Biological material

Ten males and eight females of *T. infestans* from Andean regions of Peru, South America, were obtained from the insectarium of the Faculty of Pharmaceutical Sciences, Department of Biological Sciences, UNESP, Araraquara, Brazil. The insects were obtained from a colony that was founded from seven nymphs in August 1983. Samples were used for the removal seminiferous tubules and DNA extraction. Gonads were dissected out and the tubules were directly fixed in a freshly prepared solution of methanol:acetic acid (3:1, v:v) and then stored at −20 °C. Genomic DNA was extracted from the leg muscles of males and females using the DNeasy Blood & Tissue Kit (Qiagen).

2.2. Obtaining the C_0t fraction and microlibrary construction

Repetitive DNA was isolated using renaturation kinetics (Zwick et al., 1997), with modifications, using a pool of males and females of *T. infestans*. About 10 μg DNA dissolved in 0.3 M NaCl were autoclaved at 1.4 atm (120 °C) for 15 min, and the size of fragments was checked by electrophoresis in 1% agarose. The sample was denatured at 95 °C for 10 min, placed on ice for 10 s and transferred to a water bath at 65 °C for 10 min. The sample was then incubated at 37 °C for 8 min with S1 nuclease and the reaction stopped by the addition of liquid nitrogen. DNA was purified using phenol–chloroform (1:1, v:v), and subsequently cloned using the Blunt-Ended PCR Cloning Kit (GE Healthcare Life Sciences), with *Escherichia coli* TOP10 competent cells. Six hundred fifty-three clones were used in a pre-selection by PCR with the primers M13 F (5′-GTAAAACGACG GCCAG-3′) and M13 R (5′-CAGGAAACAGCTATGAC-3′) to obtain fragments larger than 200 bp.

Inserts were sequenced on a 3500 × L automatic sequencer (Applied Biosystem), according to the manufacturer's procedures. The quality of sequences was tested with Phred-PhrapConsed software. After the identification and removal of parts of the vectors using Vector Screen (NCBI), the consensus sequences were contrasted against the NCBI (http://www.ncbi.nlm.nih.gov/blast), Flybase (http://flybase.org) and RepeatMasker (http://www.girinst.org/censor/index.php) gene banks. To get repetitive stretches, the sequences were tested with RepFind (http://cagt.bu.edu/page/REPFIND_submit) and Tandem Repeats Finder (TRF) (http://tandem.bu.edu/trf/trf.html) software.

2.3. Cytogenetics

Seminiferous tubules were incubated in 60% acetic acid for 10 min, and then minced and squashed. Coverslips were removed by freezing in liquid nitrogen. For chromosome banding (Sumner, 1982, with small modifications) all the seminiferous tubules of six males were used. Slides were aged at room temperature and also incubated in 0.2 M HCl for 10 min at room temperature, 5% barium hydroxide for 2 min at 60 °C and 2 × SSC, pH 7.0, for 60 min at 60 °C. The samples were dehydrated in an alcohol series, air dried and stained with fluorochromes: 0.5 mg/mL chromomycin A_3 (CMA_3) for 1.5 h and 2 μg/mL 4'-6-diamidino-2-phenylindole (DAPI) for 30 min. Slides were mounted with a medium composed of glycerol/McIlvaine buffer (pH 7.0) 1:1, plus 2.5 mM $MgCl_2$. After image acquisition, slides were treated with ethanol:acetic acid (3:1, v:v) for 15 min and stained with 2% Giemsa.

For FISH, the slides were prepared as previously described, and probes were labeled with biotin or digoxigenin using nick translation (Invitrogen). 18S rDNA, which was isolated from *Antiteuchus tripterus* (Bardella et al., 2013) was also labeled by nick translation, and used as control for FISH. Preparations were treated with a mixture composed of 100% formamide (15 μL), 50% polyethylene glycol (6 μL), 20 × SSC (3 μL), 100 ng sonicated calf thymus DNA (1 μL), 10% SDS (1 μL), and 100 ng probe (4 μL each). This mixture was denatured at 70 °C for 10 min, immediately chilled on ice for 5 min, and added to the slide. Chromosome denaturation/hybridization was done at 90 °C for 10 min, 48 °C for 10 min, and 38 °C for 5 min, using a thermal cycler (MJ Research, Inc., USA). Samples were incubated in a humidified chamber at 37 °C overnight. Post-hybridization washes were carried out in SSC, with 80% stringency. Probes were detected with avidin-FITC or anti-digoxigenin-rhodamine. The post-detection washes were performed in 4 × SSC/0.2% Tween 20, all at room temperature. Slides were mounted with 25 μL of a solution composed of glycerol (90%), DABCO (2.3%), 20 mM Tris–HCl, pH 8.0 (2%), 2.5 mM $MgCl_2$ (4%), and distilled water (1.7%), plus 1 μL of 2 μg/mL DAPI.

2.4. Immunolabeling

For detection of hypermethylated chromatin, seminiferous tubules were fixed in methanol–acetic acid (3:1, v:v), washed in 1 × PBS buffer, dissected in a drop of 60% acetic acid and squashed. After removing the coverslips by freezing, slides were placed in 1 × PBS for 5 min. The material was blocked in a solution of 3% BSA in 1 × PBS plus 0.2% Tween 20 (w/v) at room temperature for 10 min. Afterwards, samples were incubated with a 1:100

(v:v) solution of mouse anti-5-methylcytosine primary antibody (Eurogentec) diluted in 1 × PBS with 3% BSA plus 0.2% Tween 20 (w/v), in a moist chamber at 4 °C overnight. TRITC-conjugated goat anti-mouse secondary antibody (DAKO R0270) was used for detection.

For the detection of modified histones, H3K9me2 and H4K5ac (Feitoza and Guerra, 2011, with modifications), the seminiferous tubules were fixed in freshly prepared 4% (w/v) paraformaldehyde for 60 min at room temperature and squashed in a drop of cold 1 × PBS. After removing the coverslips by freezing, samples were blocked in a solution of 3% BSA in 1 × SSC plus 0.2% Tween 20 (w/v) at room temperature for 10 min. Afterwards, samples were incubated with anti-H4K5ac and anti-H3K9me2 antibodies (Upstate Biotechnology, USA), both diluted 1:100 in 1 × PBS with 3% BSA, in a moist chamber for 24 h at 4 °C. Samples were washed in 1 × PBS and developed with FITC-conjugated goat anti-rabbit IgG secondary antibody (Sigma), diluted 1:100 in 1 × PBS with 3% BSA, for 3 h at 37 °C. Slides were mounted as described for FISH.

2.5. Images and idiogram

Light microscopy images were acquired in grayscale using a Leica DM 4500 B microscope, equipped with a DFC 300FX camera. For FISH and immunolabeling, the images were acquired in grayscale and pseudocolored (red or blue for DAPI, greenish-yellow for FITC or TRITC and red for rhodamine) and overlapped using the Leica IM50 4.0 software. All images were optimized for best contrast and brightness using Adobe Photoshop CS software. The idiogram was organized comparing at least five doubly hybridized metaphases, using each probe, and that were subsequently treated for CMA_3/DAPI-banding.

3. Results

3.1. Conventional analysis and chromosome banding

Males of *T. infestans* from Peru showed karyotypes with $2n = 20 + XY$. The chromosomes were arranged into eight large (pairs 1–4), six medium (pairs 5–7) and six small (pairs 8–10) chromosomes plus two sex chromosomes (Fig. 1A and J). C-CMA_3/DAPI staining showed bands located preferentially in the terminal/subterminal regions of large and medium pairs and sex chromosomes. Pairs 1–4 displayed bands at both ends, with CMA_3 bands always adjacent and more internally located in relation to DAPI bands, except for pair 4, which showed a heteromorphism with only one CMA_3 band on one end of one homologous chromosome (Fig. 1B–D and J). Pairs 5 and 6 exhibited only a terminal DAPI band on one end and pair 7 showed a heteromorphism between homologous chromosomes, with one DAPI band terminal and the other intercalary (Fig. 1B–D and J). Pairs 8–10 exhibited no bands. The sex chromosomes showed differences in size. The X chromosome was the larger and displayed two DAPI bands at both ends, while the smaller Y showed a large DAPI band, which occupied more than half the length of the chromosome (Fig. 1B–D and J). To recognize the sex chromosomes, C-CMA_3/DAPI staining was performed in ganglions of eggs, where the X chromosomes showed DAPI bands at both ends (data not shown).

3.2. C_0t microlibrary

It was produced a microlibrary containing 653 clones, and these, 97 clones with inserts over than 200 bp length were chosen for sequencing. Fifty-nine of them (60.82%) displayed a tandem repetitive sequence of 79 bp length. The p*Ti*-103 clone stood out because it possessed 9.6 copies of repeats with 79 bp containing 30% A, 19% C, 21% G and 29% T (Fig. 2A). This AT-rich repeated family did not show identity with other sequences deposited in databases until now. The TRF software produced a consensus sequence for the clone p*Ti*-103, which differed from other clones only by 6% mismatches and 1% indels (Fig. 2A).

The p*Ti*-95 clone with a length of 536 bp (Fig. 3A) showed two repeats of 79 bp with high identity as those described above, directly adjacent to a stretch of 370 bp with 67% identity (*E-value* of 5e-14) for the Polinton-1_Deu of *Drosophyla eugracilis* (Fig. 3A). The 370-bp stretch was used to search protein domains to determine its location in the complete sequence of Polinton-1_Deu, which we used as a reference. The search in the Blast*p* showed of 92% identity (*E-value* of 4e-54) to an ATPase domain of the Maverick Polinton of the wasp *Cortesia congregata*, gi|531033916 (Fig. 3B). Another clone, p*Ti*-34 clone with a length 336 bp (Fig. 3C), also showed a stretch of 85 bp with 73% identity (*E-value* of 0.099) to Polinton-1 HM of the cnidarian *Hydra magnipapillata* (Fig. 3C). Although these segments are small in relation to the large size of Polintons (⩾20 kb), the recurrent appearance of stretches of these Polintons adjacent to 79 bp repetitive family did not seem to be a coincidence.

Seven clones from the microlibrary (7.22%) exhibited a tandem repetitive sequence of 33 bp length. The p*Ti*-78 was one of these clones, with 42% A, 14% C, 17% G and 26% T (Fig. 2B). The analysis using the TRF software produced a consensus sequence for the p*Ti*-78 clone, which differed from other motifs by 6% mismatches and 1% indels (Fig. 2B). Interestingly, two clones containing the 33 bp repetitive family (p*Ti*-399 and p*Ti*-646) exhibited adjacent fragments or entire sequences identical to those of the 79 bp repetitive family (described above). It was more evident in the p*Ti*-646 clone, which was 282 bp length with 26% A, 21% C, 13% G and 40% T, and had a consensus sequence with 7% mismatches and 0 indels (Fig. 2C). It showed that these repetitive families are co-located and interspersed in chromosomes. The sequences with 79 and 33 bp exhibited no identity with each other. The p*Ti*-382 clone with a length of 225 bp exhibited an 8 bp tandem repetitive motif, with 27 occurrences and 38% A, 28% C, 1% G and 33% T. The TRF software produced an AT-rich consensus sequence with 18% mismatches and 0 indel (Fig. 2D).

3.3. FISH and immunolabeling

Probes from five clones (p*At*05, p*Ti*-103, p*Ti*-95, p*Ti*-78 and p*Ti*-382) were used to generate markers in the mitotic chromosomes of *T. infestans*. The p*At*05 clone containing the 18S rDNA showed a hybridization signal at one end of pair 4 (Fig. 1E and J). The p*Ti*-78 probe containing motifs of 33 bp hybridized in both terminal regions of pairs 1 and 2, at one end of pairs 4 and 5 and on the X chromosome (Fig. 1F, H and J). The p*Ti*-103 probe with motifs of 79 bp hybridized in both terminal regions of pairs 1, 2 and 3, and the X chromosome (Fig. 1G, H and J). Hybridization signals were also detected in one terminal region of pairs 4 and 5 (Fig. 1G, H and J). The p*Ti*-95 probe produced signals in the same that p*Ti*-103 probe (data not shown). The p*Ti*-382 probe hybridized in one of the terminal regions of pairs 2 and 3 (Fig. 1I and J).

Because the p*Ti*-646 clone has shown the motifs with 79 and 33 bp positioned immediately adjacent in the insert, we performed FISH with the p*Ti*-103 and p*Ti*-78 probes in the diffuse stage at prophase I of meiosis to detect the accurate co-location of these satDNA families. The slightly condensed state of chromatin in early meiotic prophase, allowed to detect completely independent signals with the p*Ti*-78 probe (Fig. 4A–B (box) and D), as well as the accurate co-location in at least at four positions in prophase cells (Fig. 4B–C, E–F). This co-location was also observed in the nuclei of spermatocytes, when all

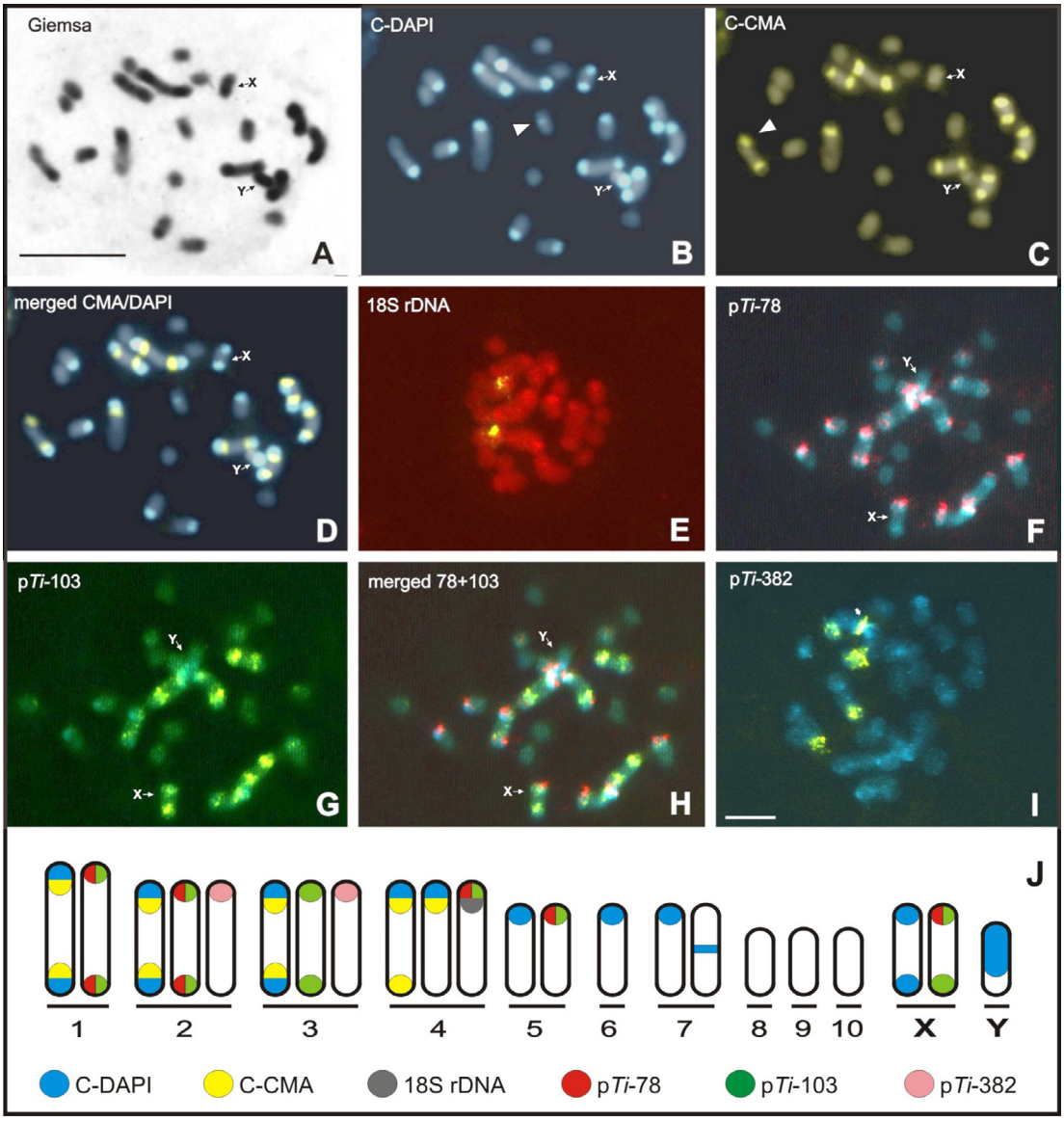

Fig. 1. Chromosome mapping in spermatogonial metaphases of *Triatoma infestans*. (A) Chromosome stained with 2% Giemsa. (B) C-DAPI banding. Note one chromosome of pair 7 with a interstitial band (arrowhead). The X chromosome presented DAPI$^+$ bands on each chromosomal end, while the Y chromosome is almost entirely DAPI$^+$. (C) C-CMA_3 banding. Note CMA_3^+ bands at subterminal regions in the pairs 1–4, as well as the absence of bands in the sex chromosomes. Observe also a heteromorphism in pair four (arrowhead). (D) C-CMA_3/DAPI band overlapping. Note the adjacent positioning of bands with those CMA_3 more internally located in relation to DAPI bands. (E) FISH with 18S rDNA (p*At*05). Ribosomal signals were detected at subterminal region of pair 4. (F) FISH with p*Ti*-78 probe showing a terminal distribution in pairs 1, 2, 4, 5 and X chromosome. (G) FISH with p*Ti*-103 probe showing a terminal distribution in pairs 1, 2, 3, 4, 5 and X chromosome. (H) Overlap of the images F and G showing the adjacent and independent positioning of 33 and 79 bp motifs at chromosome ends, respectively. (I) FISH with p*Ti*-382 at one end of pairs 2 and 3. (J) Idiogram showing all chromosome signals in *T. infestans*. Bar = 5 μm.

heterochromatic regions appeared to be associated, creating one single chromocenter (Fig. 5A–B, box).

Spermatocytes exhibited one or two chromocenters concentrating all heterochromatic regions in a "bouquet-like" structure (Fig. 5A–B). This highly methylated chromocenter was certified after immunolabeling using anti-5-methylcytosine (Fig. 5C–D), and also in subterminal and terminal chromosome regions of autosomes and sex chromosomes (Fig. 5I–K). This idea was also supported by the spermatocyte immunolabeling results, using the H3K9me2 and H4K5ac antibodies against modified histones typical of heterochromatin and euchromatin, respectively. In this case, the chromocenters evidenced by DAPI (Fig. 5E, G) appeared immunolabeled with anti-H3K9me2 but not with anti-H4K5me (Fig. 5F–H).

4. Discussion

Heteroptera exhibits chromosome numbers varying from 2 until 80, but the subfamily Triatominae is differentiated within this suborder of insects because a chromosome number of $2n = 20 + XY$ or XX is maintained with small variations related to sex system (Ueshima, 1979). Intra- and interspecific variations in chromosome sizes are associated with the accumulation of heterochromatin, which can be in one or both chromosome ends (Panzera et al., 1992, 1995). Our results using samples of *T. infestans* from the Andes exhibited a large number of terminal bands (14–20), including those of the sex chromosomes as proposed in the literature (Panzera et al., 2004). Our analysis allowed a better definition of the karyotype of *T. infestans*. We found it arranged into

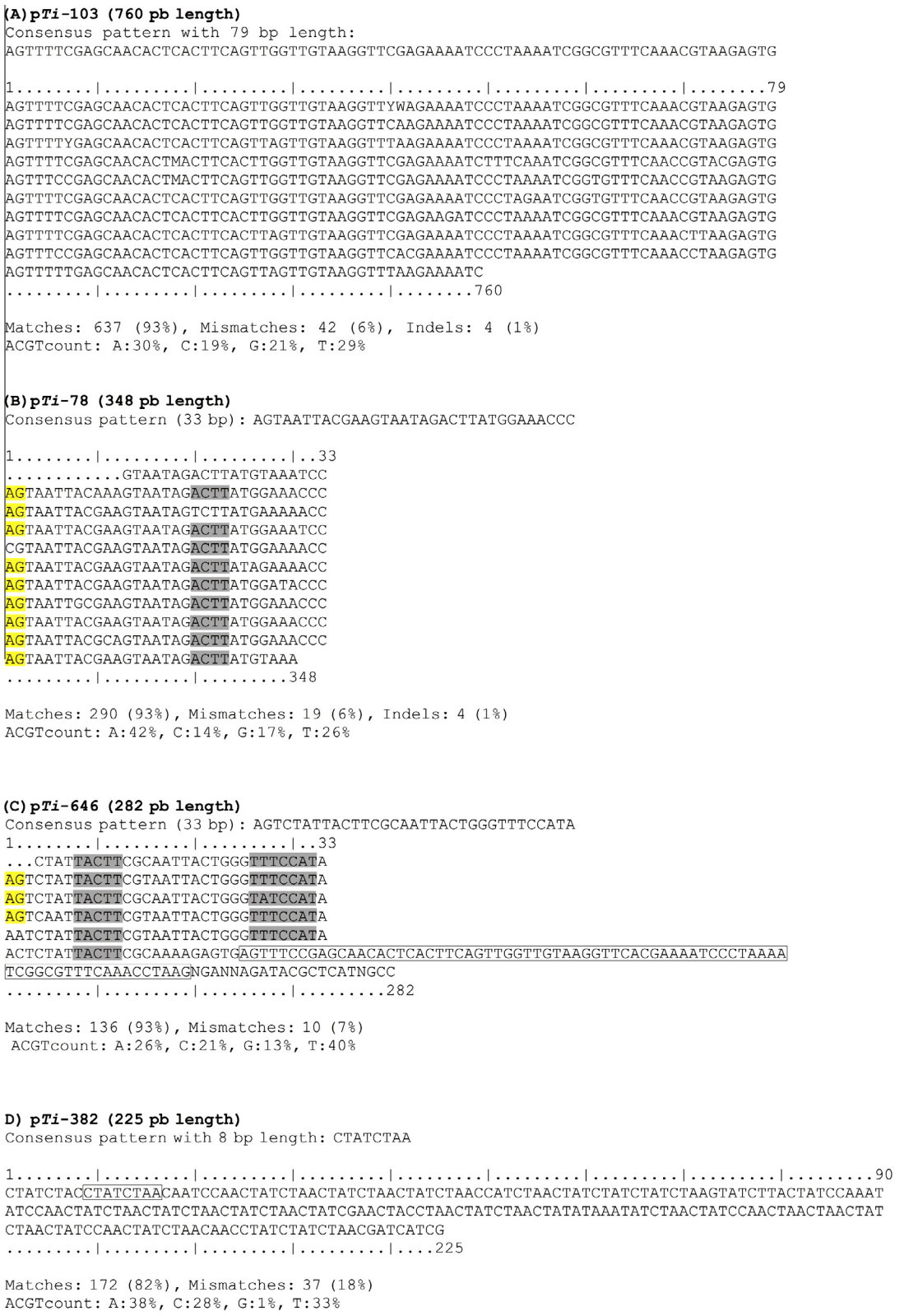

Fig. 2. Information on the sequences obtained from the clones of C_0t microlibrary of *T. infestans*. (A) Sequence of p*Ti*-103 clone with 760 bp length showing a tandemly repeated of 79 bp. Note the predominance of A and T bases. (B) Sequence of p*Ti*-78 clone with 348 bp length showing a tandemly repeated of 33 bp. Note also the predominance of A and T bases. (C) Sequence of p*Ti*-646 clone with of length 282 bp. Note that tandemly repeated sequence with 33 bp motifs is immediately adjacent to 79 bp motif (box). Highlighting in yellow in the clones p*Ti*-78 and p*Ti*-646 identifies the conserved region 5'-AG, and highlighting in gray corresponds to sequences related to Polinton elongation. (D) Sequence of p*Ti*-382 clone with length of 225 bp, which contains a AT-rich CTATCTAA (box) motif 27 times repeatedly. (For interpretation of the references to color in this figure legend, the reader is referred to the web version of this article.)

Fig. 3. Information on the sequences obtained from the clones of C_0t microlibrary of *T. infestans*. (A) Sequence of p*Ti*-95 clone with 536 bp length. The gray and yellow colors are indicating two adjacent stretches, 79 and 370 bp, respectively. The last sequence (370 bp) exibits 67% of identity with Polinton-1_Deu of *D. eugracilis* (Kojima and Jurka, 2012), separated by 26 bp. (B) Scheme showing the positioning of ATPase gene in a partial organization of Polinton of *Cortesia congregate*, whose protein domain have identity with the fragment of 370 bp of p*Ti*-95 clone. Different amino acids between sequences are represented with gray box. (C) Sequence of p*Ti*-34 clone with length of 336 bp. The yellow box highlights a 85 bp length sequence that shows 73% similarity with a Polinton-1_HM of *Hydra magnipapillata* (Bao and Jurka, 2008). (For interpretation of the references to color in this figure legend, the reader is referred to the web version of this article.)

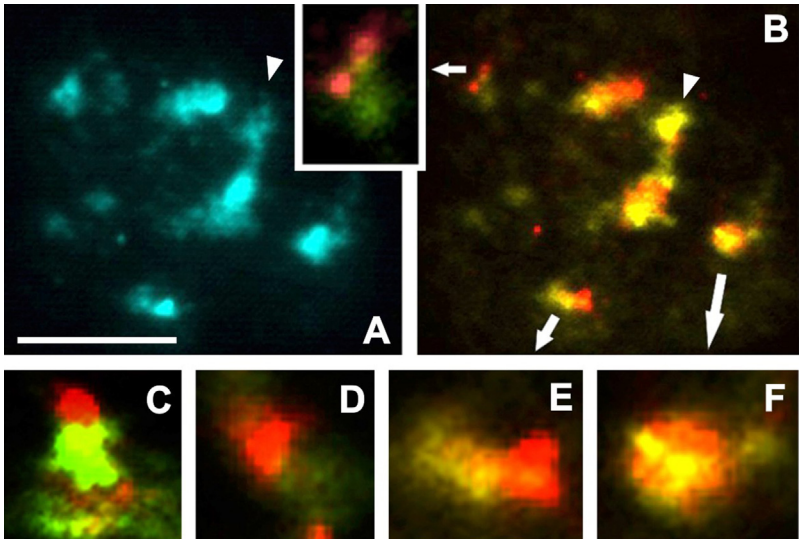

Fig. 4. Location of probes p*Ti*-78 and p*Ti*-103 in the diffuse stage chromatin of prophase I of *Triatoma infestans*. (A) DAPI staining. (B) Double FISH using the p*Ti*-103 and p*Ti*-78 probes. Arrowhead indicates a terminal chromosome region that presents a yellow signal referent to the 79 bp motif (p*Ti*-103 probe). Note in the top box another terminal chromosome region containing only red signals relative to 33 bp of p*Ti*-78 clone. (C–F) Boxes with high magnification that are showing co-locations between sequences of 33 and 79 bp after FISH. Arrows in B indicate part of two bivalents labeled by probes. Bar = 5 μm. (For interpretation of the references to color in this figure legend, the reader is referred to the web version of this article.)

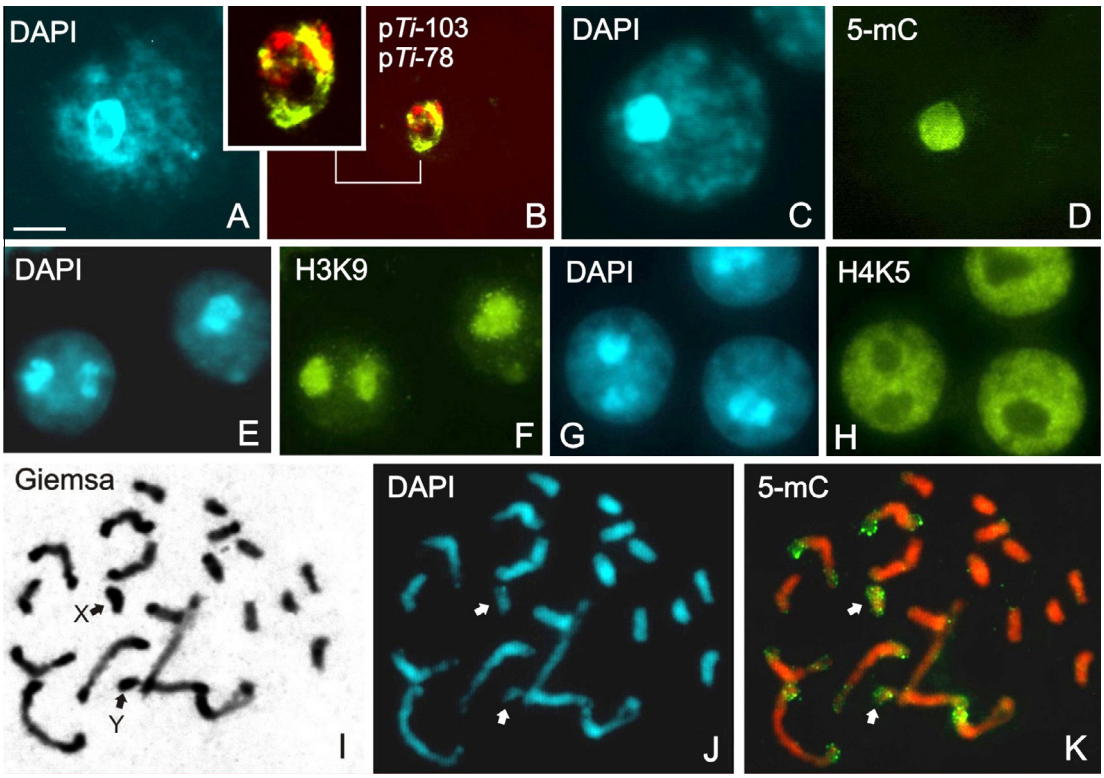

Fig. 5. Composition and heterochromatic behavior in spermatocytes of *Triatoma infestans*. (A–B) FISH using the p*Ti*-103 and p*Ti*-78 probes in spermatocytes of *T. infestans*. (A) DAPI staining and (B) chromocenter hybridized with both probes. Note regions with co-location of signals (top of chromocenter) and only with 79 bp motifs (yellowish green) on down of chromocenter (see the box). (C, E and G) Spermatocytes counterstained with DAPI. (D) Immunolabeling with anti-5mC. Note the hypermethylated chromocenters. (F) Immunolabeling with anti-H3K9. Note the strong signals in chromocenters. (H) Immunolabeling with anti-H4K5ac. Note absence of signal in chromocenters. (I) Mitotic metaphase with C-banding stained with 2% Giemsa. (J) C-Mitotic metaphase counterstained with DAPI. (K) Immunolabeling with anti-5mC. Note the signals of hypermethylation at the end of chromosomes and in almost all the sex chromosomes (arrows in I, J and K). Bar = 5 μm. (For interpretation of the references to color in this figure legend, the reader is referred to the web version of this article.)

four large, three medium and three small pairs, and two sex chromosomes, the X being slightly longer than Y. Although Panzera et al. (2004) have reported the occurrence of heterochromatic bands in both sex chromosomes, there was not a perfect definition to differentiate each sex chromosomes based in the bands profile. Our results, using chromosome banding in embryonic ganglia of samples from Peru, allowed to visualize that X chromosome was always bigger than Y, due to differential accumulation of heterochromatin.

In 25 species of Pentatomomorpha, the 18S rDNA sites were mainly located in one autosomal pair (Bardella et al., 2013). However, the species of the genus *Triatoma* exhibit high variability in the number and location of rDNA sites, presenting them in one or both sex chromosomes, as well as in one pair of autosomes (Panzera et al., 2012). The Andean (Peru) samples of *T. infestans* here studied exhibited the 18S rDNA sites in the terminal region of fourth autosomal pair, similar as reported in Bolivian samples (Panzera et al., 2012). However non-Andean samples showed hybridization signals in the X chromosome, as previously suggested by Bardella et al. (2010) and Panzera et al. (2012). This study confirm the sticking polymorphism of 18S rDNA loci in *T. infestans*.

Seven chromosome profiles were observed according to distribution and co-location of repetitive DNA families, which were: i) without bands (pairs 8, 9 and 10), ii) only with DAPI bands (pairs 6, 7 and Y), iii) with CMA_3/DAPI bands co-locating with p*Ti*-78/p*Ti*-103 signals (pair 1), iv) with CMA_3/DAPI bands co-locating with p*Ti*-78/p*Ti*-103/18S rDNA signals (pair 4), v) with CMA_3/DAPI bands co-locating with p*Ti*-78/p*Ti*-103/p*Ti*-382 signals (pair 2), vi) with CMA_3/DAPI bands co-locating with p*Ti*-103/p*Ti*-382 signals (pair 3), and vii) with DAPI bands co-locating with p*Ti*-78/p*Ti*-103 signals (pair 5 and X chromosome). The complexity in the occurrence and distribution of satDNA families in the heterochromatic regions of *T. infestans* shows that each repetitive DNA family can present distinct and independent levels of amplification/reduction and dispersion along the karyotype. These results reinforce the idea that heterochromatin is more dynamic than the euchromatic fraction in relation to the process of karyotypes differentiation among populations of *T. infestans* in South America (Panzera et al., 1995). An example of differential distribution of satDNA families along karyotypes was described in *Ixodes scapularis* (Acari – Ixodida), where AT-rich satDNA was preferentially located at terminal positions (ISR-1 and 2) on the chromosomes, with one pair bearing an interstitial site with ISR-3 (Meyer et al., 2010).

Examples such as these of *T. infestans* and *I. scapularis,* which show the sharing of specific chromosomal regions with different types of satDNA, or of *Megoura viciae* (Aphididae) where the heterochromatin is restricted to the X chromosome (Bizzaro et al., 1996), or still of *C. americana* (leaf beetle) which display the same satDNA in all chromosomes of complement (Lorite et al., 2001), could demonstrate the immense variability of behavior and distribution of satDNA in insects. Especially for co-location of different repetitive DNA families, *T. infestans* seems to be a good example because different kinds of AT-rich satDNA were found co-locate with 18S rDNA, microsatellites and transposable elements, as showed herein.

The sequence of the p*Ti*-95 clone showed two tandem DNA families, namely the satDNA of 79 bp immediately adjacent to the other sequence 370 bp in length, which exhibited identity to a stretch of Polinton-1_Deu of *Drosophila* and to a stretch of the

ATPase gene from the Maverick-like polinton of *C. congregata*. The literature contains some examples of co-location of satDNA with transposable elements. In *Drosophila melanogaster*, for instance, some classes of TEs such as *copia*, *gypsy*, *element G* and *Bari-1*, are located in the heterochromatin of autosomes and sex chromosomes (Pimpinelli et al., 1995). This was also observed in vertebrates (cichlids), where *Rex* retrotransposons are found co-locating with pericentromeric heterochromatin (Valente et al., 2011).

The p*Ti*-78 clone was particularly interesting because the 33-bp motif exhibited identity with the TIRs of Polintons. These regions show a universal fragment 5'-AG (Kapitonov and Jurka, 2007; Pritham et al., 2007), which was also identified in the 33-bp motifs of seven clones, represented here by the p*Ti*-78 and p*Ti*-646 clones. Besides, the motif of clone p*Ti*-78 showed a TTTCAT fragment that was duplicated, inverted and internally positioned in the 33 bp motif. This drew our attention because the presence of two T residues in the TTTCAT motif is one of the determinant factors for elongation of Polintons by polymerase B (Méndez et al., 1992). In the p*Ti*-646 clone, for instance, we found two internal motifs (TACTTC and TTTCCAT) separated by 12 nucleotides. The substitution of T by C in the first fragment and the addition of a C in the second fragment could be enough to initiate a sliding-back replication, which may explain the tandem amplification of the 33-bp DNA family in *T. infestans*. This case could be similar to that described by Méndez et al. (1992) for bacteriophage ϕ29. The origin of satDNAs from TIRs or other fragments of transposable elements has been previously reported in the literature. In the coleopteran *Misolampus goudoti*, for example, two satDNA families (*Eco*RI with 196 bp and *Psd*I with 1.2 kb), showed similarity with TIRs of class II transposable elements (Pons, 2004).

Another fact that drew out attention is the short length of the motifs of the clones p*Ti*-103 (79 bp), p*Ti*-78 and p*Ti*-646 (33 bp) and p*Ti*-382 (8 bp). The satDNA sequences of more than 100 bp in length seem to be more common in plants and animals (Heslop-Harrison and Schwarzacher, 2011; Palomeque and Lorite, 2008). As examples we can mention the 180 bp repeat of *Eyprepocnemis plorans*, Orthoptera (López-León et al., 1995) and 189 bp repeat of *Myzus persicae*, Hemiptera (Mandrioli et al., 1999), and some are even much larger, such as the 1.2 kb repeat described for *M. goudoti*, Coleoptera (Pons, 2004). But short motifs, such as the AT-rich satDNA reported here for *T. infestans*, were also reported for *Messor structor*, Hymenoptera, whose motif showed a length of 79 bp (Lorite et al., 1999), and *Anopheles gambiae*, Diptera, with a length of 53 bp (Krzywinski et al., 2005). At least for *T. infestans*, these short motifs may have originated and amplified from Polintons, arranging the end the AT-rich heterochromatin. This idea is reinforced by AT-rich chromosomal regions that show the main cytological features defining heterochromatin, such as hypermethylation and lack of euchromatin, which were recognized here by immunolabeling with anti-5-Mc, anti-H3K9me2 and anti-H4K5ac, respectively. Evidences produced after immunolabeling with anti-H3K9me2 antibody showed that the heterochromatic regions in insects, such as *Mamestra brassicae* (Lepidoptera) and *Acyrthosiphon pisum* (Aphididae), are also rich in lysine-methylated histone H3 (Borsatti and Mandrioli, 2005; Mandrioli and Borsatti, 2007).

The variability in chromosome band patterns between distinct populations of *T. infestans* is well documented in the literature (Panzera et al., 1995, 2004). However, the origin of this variability is poorly understood. Besides learning a little more about the origin of the AT-rich portion in *T. infestans*, our study produced new chromosome markers that can be used to check the dynamics of rearrangements that play a role in karyotype differentiation in this species, as well as in other species of the genus *Triatoma*. Besides evidence of the participation of a Polinton-like element in the origin of AT-rich repeat arrays in *T. infestans*, we can recognize different mechanisms of rearrangement occurring at the ends of chromosomes, such as sliding-back (33-bp motif), slippage replication (8-bp motif), amplification associated with equilocal dispersion (at the chromosome ends) and inversion (pair 7). The greatest impediment was related to obtaining the complete sequence of the Polinton, because these giant TEs have been reconstructed only in silico. Future advances in this area depend on large-scale genomic sequencing to identify, characterize and certify the class or kind of Polinton-like element that now seems to be elected as the source of this large variation in AT-rich heterochromatin in *T. infestans*.

Acknowledgements

The authors thank CNPq, Fundação Araucária and CAPES for financial support, as well as Prof. Dr. Marcelo Guerra (UFPE, Brazil) for providing the antibodies and Dr. A. Leyva for English review of the manuscript.

References

Bao, W., Jurka, J., 2008. Polinton DNA transposons from *Hydra magnipapillata*. Repbase Rep. 8 (12), 2101-2101.

Bardella, V.B., Gaeta, M.L., Vanzela, A.L.L., Azeredo-Oliveira, M.T.V., 2010. Chromosomal location of heterochromatin and 45S rDNA sites in four South American triatomines (Heteroptera: Reduviidae). Comp. Cytogenet. 4, 141–149.

Bardella, V.B., Grazia, J., Fernandes, J.A.M., Vanzela, A.L.L., 2014. High diversity in CMA_3/DAPI-banding patterns in heteropterans. Cytogenet. Genome Res. 142 (1), 46–53.

Bardella, V.B., Fernandes, T., Vanzela, A.L.L., 2013. The conservation of number and location of 18S sites indicates the relative stability of rDNA in species of Pentatomomorpha (Heteroptera). Genome 56 (7), 425–429.

Bizzaro, D., Manicardi, G.C., Bianchi, U., 1996. Chromosomal localization of highly repeated *Eco*RI DNA fragment in *Megoura viciae* (Homoptera, Aphididae) by nick translation and fluorescence in situ hybridization. Chromosome Res. 4 (5), 392–396.

Borsatti, F., Mandrioli, M., 2005. Conservation of heterochromatic components and epigenetic markers in the holocentric chromosomes of the cabbage moth, *Mamestra brassicae* (Lepidoptera). Eur. J. Entomol. 102, 625–632.

Bressa, M.J., Franco, M.J., Toscani, M.Y., Papeschi, A.G., 2008. Heterochromatin heteromorphism in *Holhymenia rubiginosa* (Heteroptera: Coreidae). Eur. J. Entomol. 105, 65–72.

Cabral-de-Mello, D.C., Moura, R.C., Carvalho, R., Souza, M.J., 2010. Cytogenetic analysis of two related *Deltochilum* (Coleoptera, Scarabaeidae) species: diploid number reduction, extensive heterochromatin addition and differentiation. Micron 41, 112–117.

Feitoza, L., Guerra, M., 2011. Different types of plant chromatin associated with modified histones H3 and H4 and methylated DNA. Genetica 139, 305–314.

Heslop-Harrison, J.S., Schwarzacher, T., 2011. Organisation of plant genome in chromosomes. Plant J. 66, 18–33.

Kapitonov, V.V., Jurka, J., 2007. Self-synthesizing DNA transposons in eukaryotes. Proc. Natl. Acad. Sci. 103, 4540–4545.

Kojima, K.K., Jurka, J., 2012. Polintons from the *Drosophila eugracilis* genome. Repbase Rep. 12 (6), 996-996.

Krzywinski, J., Sangare, D., Besansky, N.J., 2005. Satellite DNA from the Y chromosome of the malaria vector *Anopheles gambiae*. Genetics 169, 185–196.

López-León, M.D., Vazquez, P., Hewitt, G.M., Camacho, J.P., 1995. Cloning and sequence analysis of an extremely homogeneous tandemly repeated DNA in the grasshopper *Eyprepocnemis plorans*. Heredity 75, 370–375.

Lorite, P., García, M.F., Palomeque, T., 1999. Satellite DNA in the ant *Messor structor* (Hymenoptera, Formicidae). Genome 42, 881–886.

Lorite, P., Palomeque, T., Garnería, I., Petitpierre, E., 2001. Characterization and chromosome location of satellite DNA in the leaf beetle *Chrysolina americana* (Coleoptera, Chrysomelidae). Genetica 110, 143–150.

Mandrioli, M., Bizzaro, D., Manicardi, G.C., Gionghi, D., Bassoli, L., et al., 1999. Cytogenetic and molecular characterization of a highly repeated DNA sequence in the peach potato aphid *Myzus persicae*. Chromosoma 108, 436–442.

Mandrioli, M., Borsatti, F., 2007. Analysis of heterochromatin epigenetic markers in the holocentric chromosomes of the aphid *Acyrthosiphon pisum*. Chromosome Res. 15, 1015–1022.

Méndez, J., Blanco, L., Esteban, J.A., Bernad, A., Salas, M., 1992. Initiation of ϕ29 DNA replication occurs at the second 3' nucleotide of the linear template: a sliding-back mechanism for protein-primed DNA replication. Proc. Natl. Acad. Sci. 89, 9579–9583.

Meyer, J.M., Kurtti, T.J., Zee, J.P.V., Hill, C.A., 2010. Genome organization of major tandem repeats in the hard tick *Ixodes scapularis*. Chromosome Res. 18, 357–370.

Palomeque, T., Lorite, P., 2008. Satellite DNA in insects: a review. Heredity 100, 564–573.

Panzera, F., Alvarez, F., Sanchez-Rufas, J., Pérez, R., Suja, J.A., et al., 1992. C-heterochromatin polymorphism in holocentric chromosomes of *Triatoma infestans* (Hemiptera-Reduviidae). Genome 35, 1068–1074.

Panzera, F., Pérez, R., Panzera, Y., Alvarez, F., Scvortzoff, E., et al., 1995. Karyotype evolution in holocentric chromosomes of three related species of triatomines (Hemiptera-Reduviidae). Chromosome Res. 3 (3), 143–150.

Panzera, F., Pérez, R., Hornos, S., Panzera, Y., Cestau, R., et al., 1996. Chromosome number in the Triatominae (Hemiptera – Reduviidae): a review. Mem. Inst. Oswaldo Cruz 91, 515–518.

Panzera, F., Dujardin, J.P., Nicolini, P., Caraccio, M.N., Rose, V., et al., 2004. Genomic changes of Chagas disease vector South America. Emerg. Infect. Dis. 10 (3), 438–446.

Panzera, F., Pérez, R., Panzera, Y., Ferrandis, I., Ferreiro, M.J., et al., 2010. Cytogenetics and genome evolution in the subfamily Triatominae (Hemiptera, Reduviidae). Cytogenet. Genome Res. 128, 77–87.

Panzera, Y., Pita, S., Ferreiro, M.J., Ferrandis, I., Lages, C., et al., 2012. High dynamics of rDNA cluster location in kissing bug holocentric chromosomes. Cytogenet. Genome Res. 138, 56–67.

Pérez, R., Rufas, J., Suja, J., Panzera, F., 2000. Meiosis in holocentric chromosomes: orientation and segregation of an autosome and sex chromosomes in *Triatoma infestans*. (Heteroptera). Chromosome Res. 8, 17–25.

Pimpinelli, S., Berloco, M., Fanti, L., Dimitri, P., Bonaccorsi, S., et al., 1995. Transposable elements are stable structural components of *Drosophila melanogaster* heterochromatin. Proc. Natl. Acad. Sci. 92, 3804–3808.

Plohl, M., Mestrovic, N., Bruvo, B., Ugarkovic, D., 1998. Similarity of structural features and evolution of satellite DNAs from *Palorus subdepressus* (Coleoptera) and related species. J. Mol. Evol. 46, 234–239.

Pons, J., 2004. Cloning and characterization of a transposable-like repeat in the heterochromatin of the darkling beetle *Misolampus goudoti*. Genome 47, 769–774.

Pritham, E.J., Putliwala, T., Feschotte, C., 2007. *Mavericks*, a novel class of giant transposable elements widespread in eukaryotes and related to DNA viruses. Gene 390, 3–17.

Schmidt, T., Heslop-Harrison, J.S., 1998. Genomes, genes and junk: the large-scale organization of plant chromosomes. Trends Plant Sci. 3, 195–199.

Schneider, M.C., Almeida, M.C., Rosa, S.P., Costa, C., Cella, D.M., 2006. Evolutionary chromosomal differentiation among four species of *Conoderus* Eschscholts, 1829 (Coleoptera, Elateridae, Agrypninae, Conoderini) detected by standard staining, C-banding, silver nitrate impregnation, and CMA_3/DA/DAPI staining. Genetica 128, 333–346.

Subirana, J.A., Messeguer, X., 2013. A satellite explosion in the genome of holocentric nematodes. PLoS One 8 (4), e62221.

Sumner, A.T., 1982. The nature and mechanisms of chromosome banding. Cancer Genet. Cytogenet. 6, 59–87.

Ueshima, N., 1979. Hemiptera II: Heteroptera. In: John, B. (Ed.), Animal Cytogenetics. 3. Insecta 6. Gebrüder Bornträger, Berlin, Stuttgart, p. 113.

Valente, G.T., Mazzuchelli, J., Ferreira, I.A., Poletto, A.B., Fantinatti, B.E.A., et al., 2011. Cytogenetic mapping of the retroelements *Rex1*, *Rex3* and *Rex6* among cichlid fish: new insights on the chromosomal distribution of transposable elements. Cytogenet. Genome Res. 133, 34–42.

Zwick, M.S., Hanson, R.E., Islam-Faridi, M.N., Stelly, D.M., Wing, R.A., et al., 1997. A rapid procedure for the isolation of C_0t–1 DNA from plants. Genome 40, 138–142.